Supporting Information for

Linear and branched supramolecular polymers formed from isomeric monomers as revealed by solution viscoelasticity

Yufuka Furukawa,[a†] Ren Sato,[b†] Natsumi Fukaya,[a] Takashi Kajitani,[c] Takuya Katashima*[,b] and Kazunori Sugiyasu*[,a]

[a]Department of Polymer Chemistry, Graduate School of Engineering, Kyoto University, Kyotodaigaku-katsura, Saikyo-ku, Kyoto 615-8510, Japan
[b]Department of Bioengineering, Graduate School of Engineering, The University of Tokyo, 7-3-1 Hongo, Bunkyo-ku, Tokyo 113-8656, Japan
[c]Core Facility Center, Research Infrastructure Management Center, Institute of Science Tokyo, 4259 Nagatsuta, Midori-ku, Yokohama 226-8501, Japan
[†]These authors contribute equally to this work.

*katashima@g.ecc.u-tokyo.ac.jp, sugiyasu.kazunori.8z@kyoto-u.ac.jp

Table of contents

1. Experimental Section

1.1 General

^{1}H and ^{13}C NMR spectra were recorded with a JEOL AL-400 spectrometer (400 MHz for ^{1}H, 100 MHz for ^{13}C) or JEOL JNM-ECS400 (400 MHz for ^{1}H, 100 MHz for ^{13}C) in $CDCl_3$. The chemical shifts in ^{1}H NMR spectra are reported in δ ppm using the residual protons of the solvents as an internal standard (trimethylsilane δ 0.00), and those in ^{13}C NMR spectra are reported using the solvent signal as an internal standard ($CHCl_3$ δ 77.16). Mass spectra were measured with a Thermo Fisher Scientific Exactive Plus Orbitrap MS System with the ionization methods of electrospray ionization (ESI). Thin layer chromatography (TLC) was performed on glass plates coated with 0.25 mm thickness of silica gel $60F_{254}$ (Merck). Column chromatography was performed using silica gel PSQ100B (Fuji Silysia Chemicals). All chemicals were purchased from commercial suppliers and used without further purification. Anhydrous DMF was purchased from Kanto Chemicals and further purified by Glass Contour Solvent Systems. 2-decyltetradecyl 4-methylbenzenesulfonate[S1] was synthesized according to the reported procedures. All reactions were performed with dry glassware and under a nitrogen atmosphere unless stated otherwise.

1.2 Preparation of a solution of DT_{34} or DT_{35} in dodecane

Compound **DT_{34}** or **DT_{35}** was dissolved in *n*-dodecane with desired concentration. The resulting solution was heated to a temperature above 353 K by using a heat gun and cooled at around 293 K for 30 min to afford supramolecular polymer of **D_{345}**, **DT_{34}** or **DT_{35}**.

1.3 Spectroscopy

The spectroscopic measurements were conducted under ambient conditions using solvents of spectroscopic grade. Fourier transform infrared (FT-IR) spectroscopic analysis was

performed on a Thermo Fisher Sciectific Nicolet iS50 spectrometer. UV-vis absorption spectra were recorded using a quartz cuvette of 2 mm path length with a JASCO V-750 spectrophotometer equipped with a JASCO ETCR-762 cell holder for temperature control.

1.4 Scanning Electron Microscopy

Scanning Electron Microscopy (SEM) measurements were performed on a HITACHI, FE-SEM: Regulus 8220. Sample was mounted on a glass slide attached to a SEM stage by conducting carbon tape and then coated with platinum. The images were recorded with an operating voltage of 1.0 kV.

1.5 Polarized Light Microscopy

Polarized optical microscopic (POM) measurements were performed on Evident BX53-P digital microscope.

1.6 Small- and Wide-Angle X-Ray Scattering

SAXS and WAXS of gel and solution samples were measured in a glass capillary with a diameter of 1.5 mm using a Rigaku NANOPIX equipped with a HyPix-6000 (Rigaku) detector. The scattering vector ($q = 4\pi\sin\theta/\lambda$), scattering angle θ and the position of the incident X-ray beam on the detectors were calibrated using several orders of layer reflections from silver behenate ($d = 58.380$ Å), where λ refers to the wavelength of the X-ray beam (Cu Kα, 1.54 Å). The sample-to-detector distance was approximately 100 or 470 mm. The obtained diffraction patterns were integrated along the Debye-Scherrer ring to afford 1D intensity data using the Rigaku 2DP software. The cell parameters were refined using CellCalc ver. 2.10 software. The SAXS data were analyzed using the SasView application (https://www.sasview.org).

1.7 Atomic Force Microscopy

Atomic force microscopy (AFM) was performed on a Bruker model MultiMode 8 atomic force microscope under ambient conditions in the scan assist mode. Silicon cantilevers (SCANASYST-AIR) with a spring constant of 0.4 N/m and a frequency of 70 kHz were used. The samples were spin-coated on a silicon wafer and the solvent was removed. Spin-coating was performed using an Oshigane SC-300. AFM images were analyzed with Bruker Nanoanalysis.

1.8 Linear Viscoelastic Measurements

DT$_{34}$ and **DT$_{35}$** were dissolved in *n*-dodecane at concentrations of 5 mM, 7 mM, and 10 mM. Small amplitude oscillatory shear measurements and stress relaxation tests were conducted to evaluate the storage (G') and loss (G'') moduli using a stress-controlled rheometer (MCR301, Anton Paar). A parallel plate fixture with a 25 mm diameter was used. The angular frequency dependence (from 10^{-5} to 10^{2} rad s^{-1}) of G' and G'' was measured at 25°C. The oscillatory shear strain amplitude (γ) was 0.01, confirmed beforehand to be within the linear viscoelasticity range.

Notably, G' and G'' in the low-frequency region (ω < 0.1 rad s^{-1}) were evaluated from relaxation modulus. In these calculations, G' and G'' were described using the discrete relaxation spectrum as

$$G' = \sum_p h_p \frac{\omega^2 {\tau_p}^2}{1 + \omega^2 {\tau_p}^2}$$

$$G'' = \sum_p h_p \frac{\omega \tau_p}{1 + \omega^2 {\tau_p}^2}$$

Here, h_p and τ_p represent the relaxation strength and time of the p-th component. The relaxation modulus ($G(t)$) is described as

$$G(t) = \sum_p h_p \left(1 - \exp\left(\frac{t}{\tau_p}\right)\right)$$

We numerically estimated G' and G'' from experimentally obtained $G(t)$.

2. Synthetic Procedures

2.1 Synthesis of compound D_{345}

Compound D_{345} was synthesized according to a modified procedure from the reported method. [S2]

2.2 Synthesis of compound DT_{34}

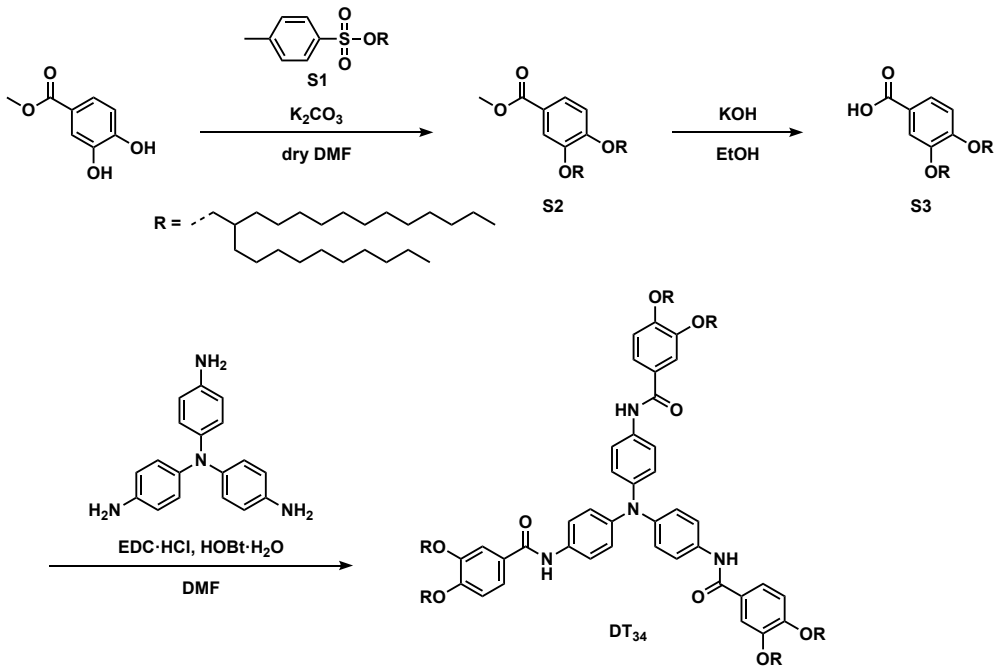

Scheme S1. Synthesis of compound **DT_{34}**.

Compound S2. 2-Decyltetradecyl 4-methylbenzenesulfonate (**S1**) (4.90 g, 9.63 mmol) was added to a solution of methyl 3,4-dihydroxybenzoate (688 mg, 4.09 mmol) and K_2CO_3 (2.65 g, 19.2 mmol) in anhydrous DMF (22 mL). The reaction mixture was stirred at 80 °C for 1 day. Distilled water was added to the resulting mixture and the aqueous layer was extracted with hexane three times. The combined organic layer was washed with water and dried over Na_2SO_4. After filtration, the solvent was removed under reduced pressure. The mixture was subjected to silica gel column chromatography using 5:1 hexane/dichloromethane mixed solvent as eluent (R_f = 0.25) to afford **S2** as a colorless oil (3.14 g, 3.73 mmol, 91%).

^{1}H NMR (400 MHz, $CDCl_3$): δ 7.62 (dd, J = 8.5, 2.1 Hz, 1H), 7.51 (d, J = 1.8 Hz, 1H), 6.84 (d, J = 8.7 Hz, 1H), 3.90–3.88 (m, 7H), 1.84–1.78 (m, 2H), 1.51–1.20 (m, 80H), 0.89–0.86 (m, 12H); ^{13}C NMR (100 MHz, $CDCl_3$): δ 167.2, 153.7, 149.1, 123.5, 122.3, 114.0, 111.8, 71.9, 71.7, 52.0, 38.3, 38.2, 32.1, 31.5, 31.5, 30.3, 30.2, 29.9, 29.9, 29.5, 27.1, 27.0, 22.9, 14.3; HRMS (ESI): m/z calcd. for $C_{56}H_{104}NaO_4$: 863.7827 ([M+Na]$^+$); found: 863.7821.

Compound S3. Potassium oxide (2.09 g, 37.2 mmol) was added to a solution of **S2** (3.21 g, 3.81 mmol) in methanol (31.5 mL) and water (5.3 mL). The reaction mixture was refluxed for 24 h under air atmosphere. An aqueous solution of HCl (1 M, 80 mL) was added to the resulting mixture and the aqueous layer was extracted with dichloromethane three times. The combined organic layer was dried over Na_2SO_4. After filtration, the solvent was removed under reduced pressure to afford **S3** as a colorless oil, which was used in the next step without further purification.

^{1}H NMR (400 MHz, $CDCl_3$): δ 7.71 (dd, J = 8.2, 1.8 Hz, 1H), 7.56 (d, J = 1.8 Hz, 1H), 6.87 (d, J = 8.2 Hz, 1H), 3.91 (t, J = 5.9 Hz, 4H), 1.88–1.77 (m, 2H), 1.55–1.18 (m, 80H), 0.88 (t, J = 6.6 Hz, 12H); ^{13}C NMR (100 MHz, $CDCl_3$): δ 171.9, 154.5, 149.1, 124.5, 121.3, 114.3, 111.7, 71.9, 71.7, 38.2, 38.1, 32.1, 31.5, 31.5, 30.3, 30.2, 29.9, 29.9, 29.5, 27.1, 27.0, 22.9, 14.3; HRMS (ESI-MS): m/z calcd. for $C_{55}H_{101}O_4$: 825.7705 ([M–H]$^-$); found: 825.7701.

Compound DT$_{34}$. Triethylamine (0.070 mL) was slowly added to a solution of **S5** (0.473 g, 0.572 mmol), tris(4-aminophenyl)amine (40.4 mg, 0.139 mmol), 1-ethyl-3-(3-dimethylaminopropyl)carbodiimide hydrochloride (EDCl·HCl) (93.8 mg, 0.489 mmol) and 1-hydroxybenzotriazole monohydrate (HOBt·H_2O) (74.8 mg, 0.488 mmol) in DMF (8 mL) in ice bath. The reaction mixture was stirred in room temperature for 1 day. Distilled water was added to the resulting mixture and the aqueous layer was extracted with 4:1 hexane/ethyl

acetate mixed solvent (35 mL). The organic layer was washed by water, saturated $NaHCO_3$ aq, and brine. The combined organic layer was dried over Na_2SO_4. After filtration, the solvent was removed under reduced pressure. The mixture was subjected to silica gel column chromatography using a 4:1 chloroform/hexane mixed solvent as eluent (R_f = 0.15) to afford **DT$_{34}$** as a white solid (0.253 g, 0.0931 mol, 67%).

^{1}H NMR (400 MHz, $CDCl_3$): δ 7.72 (s, 3H), 7.52 (d, J = 9.1 Hz, 6H), 7.45 (d, J = 1.8 Hz, 3H), 7.34 (dd, J = 8.5, 2.1 Hz, 3H), 7.09 (d, J = 8.7 Hz, 6H), 6.88 (d, J = 8.7 Hz, 3H), 3.92–3.90 (m, 12H), 1.83–1.82 (m, 6H), 1.52–1.01 (m, 240H), 0.89–0.86 (m, 36H); ^{13}C NMR (100 MHz, $CDCl_3$): δ 165.4, 152.7, 149.7, 144.2, 133.2, 127.2, 124.5, 121.6, 119.5, 112.5, 112.2, 72.0, 71.9, 38.3, 38.2, 32.1, 31.5, 30.3, 29.9, 29.8, 29.5, 27.1, 22.8, 14.3; HRMS (ESI): m/z calcd. for $C_{183}H_{318}N_4O_9Cl$: 2751.4243 ([M+Cl]$^-$); found: 2751.4297.

2.3 Synthesis of compound DT_{35}

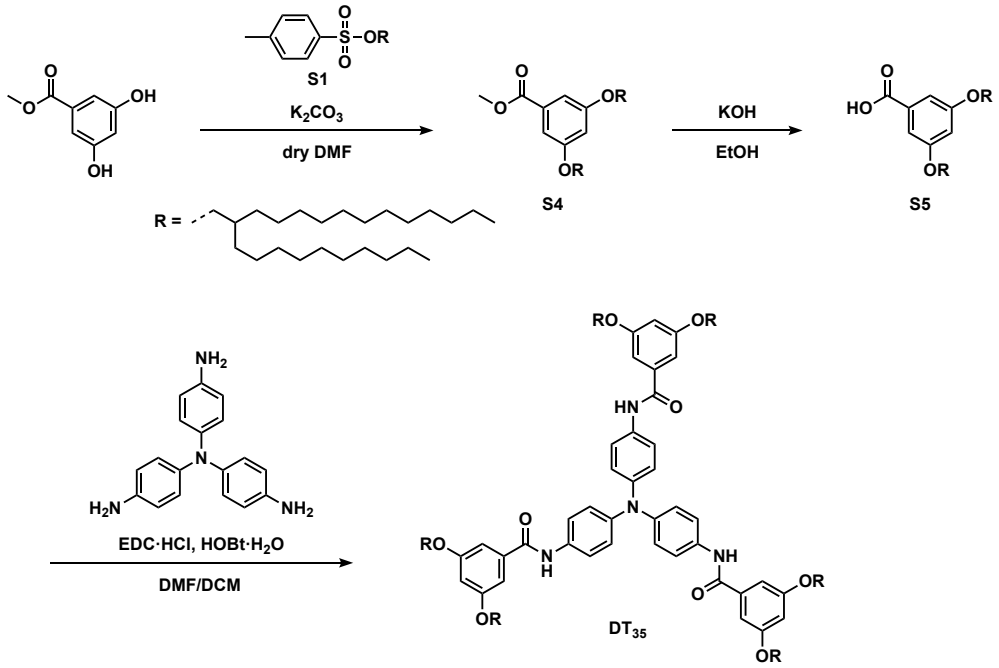

Scheme S2. Synthesis of compound **DT_{35}**.

Compound S4. Compound **S1** (5.00 g, 9.82 mmol) was added to a solution of methyl 3,5-dihydroxybenzoate (689 mg, 4.10 mmol) and K_2CO_3 (2.56 g, 18.5 mmol) in anhydrous DMF (22 mL). The reaction mixture was stirred at 80 °C for 1 day. Distilled water was added to the resulting mixture and the aqueous layer was extracted with 4:1 hexane/ethyl acetate (3 × 40 mL). The combined organic layer was washed with water and dried over Na_2SO_4. After filtration, the solvent was removed under reduced pressure. The mixture was subjected to silica gel column chromatography using 5:1 hexane/dichloromethane mixed solvent as eluent (R_f = 0.25) to afford **S4** as a colorless oil (3.36 g, 3.99 mmol, 97%).

^{1}H NMR (400 MHz, $CDCl_3$) δ 7.15 (d, J = 2.3 Hz, 2H), 6.64 (t, J = 2.3 Hz, 1H), 3.90 (s, 3H), 3.84 (d, J = 5.5 Hz, 4H), 1.77–1.71 (m, 2H), 1.51–1.06 (m, 80H), 0.88 (t, J = 6.9 Hz, 12H); ^{13}C NMR (100 MHz, $CDCl_3$) δ 167.1, 160.5, 131.8, 107.6, 106.6, 71.2, 52.2, 38.1, 32.1, 31.5,

30.2, 29.9, 29.8, 29.5, 27.0, 22.9, 14.3; HRMS (ESI): *m*/*z* calcd. for $C_{56}H_{104}NaO_4$: 863.7827 ([*M*+Na]$^+$); found: 867.7823.

Compound S5. Potassium oxide (2.22 g, 39.6 mmol) was added to a solution of **S4** (3.35 g, 3.98 mmol) in methanol (34 mL) and water (5.7 mL). The reaction mixture was refluxed for 24 h under air atmosphere. An aqueous solution of HCl (1 M, 80 mL) was added to the resulting mixture and the aqueous layer was extracted with dichloromethane three times. The combined organic layer was dried over Na_2SO_4. After filtration, the solvent was removed under reduced pressure to afford **S5** as a colorless oil, which was used in the next step without further purification.

^{1}H NMR (400 MHz, $CDCl_3$) δ 7.22 (d, J = 2.3 Hz, 2H), 6.69 (t, J = 2.3 Hz, 1H), 3.86 (d, J = 5.5 Hz, 4H), 1.79–1.75 (m, 2H), 1.47–1.20 (m, 80H), 0.88 (t, J = 6.9 Hz, 12H); ^{13}C NMR (100 MHz, $CDCl_3$) δ 160.6, 108.2, 71.3, 38.1, 32.1, 31.5, 30.2, 29.9, 29.8, 29.5, 27.0, 22.8, 14.3, 0.1; HRMS (ESI-MS): *m*/*z* calcd. for $C_{55}H_{101}O_4$: 825.7705 ([*M*–H]$^-$); found: 825.7700.

Compound DT$_{35}$. Triethylamine (0.605 mL) was slowly added to a solution of **S5** (3.58 g, 4.33 mmol), tris(4-aminophenyl)amine (363.4 mg, 1.25 mmol), EDCl·HCl (842.2 mg, 4.39 mmol) and HOBt·H_2O (666.6 mg, 4.35 mmol) in 1:1 DMF/ dichloromethane (72 mL) in ice bath. The reaction mixture was stirred in room temperature for 1 day. Distilled water was added to the resulting mixture and the aqueous layer was extracted with hexane (50 mL). The organic layer was washed by water, saturated $NaHCO_3$ aq, and brine. The combined organic layer was dried over Na_2SO_4. After filtration, the solvent was removed under reduced pressure. The mixture was subjected to silica gel column chromatography using 3:2 dichloromethane/hexane mixed solvent as eluent (R_f = 0.25) to afford **DT$_{35}$** as a white solid (2.54 g, 0.935 mol, 75%).

^{1}H NMR (400 MHz, $CDCl_3$) δ 7.71 (s, 3H), 7.53 (d, J = 9.1 Hz, 6H), 7.10 (d, J = 9.1 Hz, 6H), 6.95 (d, J = 2.3 Hz, 6H), 6.61 (t, J = 2.1 Hz, 3H), 3.87 (d, J = 5.5 Hz, 12H), 1.79–1.75 (m, 6H), 1.47-1.22 (m, 240H), 0.87 (t, J = 6.6 Hz, 36H); ^{13}C NMR (100 MHz, $CDCl_3$) δ 165.7, 160.8, 144.3, 136.9, 133.0, 124.4, 121.8, 105.4, 104.8, 71.2, 38.1, 32.1, 31.4, 30.2, 29.9, 29.8, 29.5, 27.0, 22.8, 14.2; HRMS (ESI): m/z calcd. for $C_{183}H_{318}N_4NaO_9$: 2739.4441 ($[M+Na]^+$); found: 2739.4391.

3. Supplementary Figures

3.1 Self-assembly Behavior

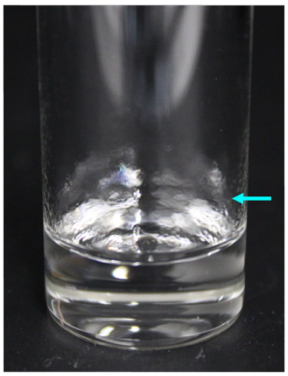

Figure S1. Photograph of a dodecane solution of $\mathbf{D_{345}}$ at a concentration of 5.0×10^{-5} M. The blue arrow highlights the presence of precipitates.

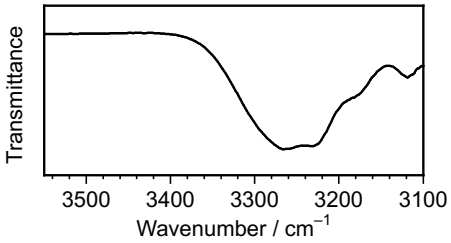

Figure S2. FT-IR spectrum of a solution of $\mathbf{D_{345}}$ at a concentration of 10 mM in dodecane.

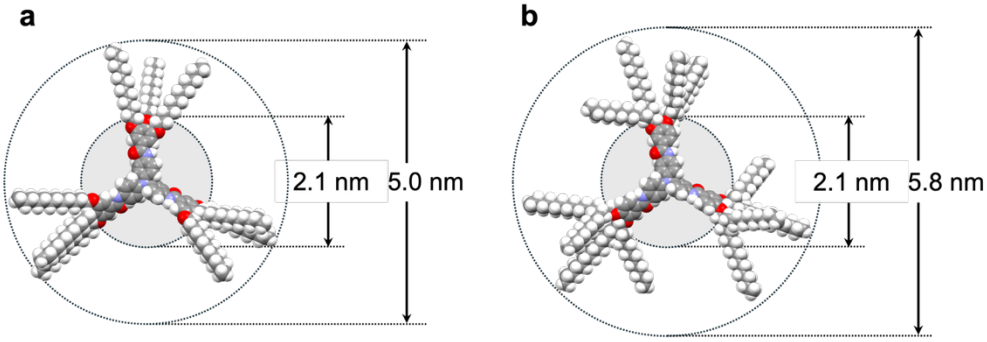

Figure S3. Molecular models of (a) **D**$_{345}$ and **DT**$_{34}$.

Table S1. Structural Parameters Obtained from Cylinder Model Fitting with SAXS Data

	c (mM)	D_{Ave} (nm)	L_{pAve} (nm)
D$_{345}$	10	6.667	23.16
DT$_{34}$	10	2.805	17.71
DT$_{35}$	10	2.652	16.94

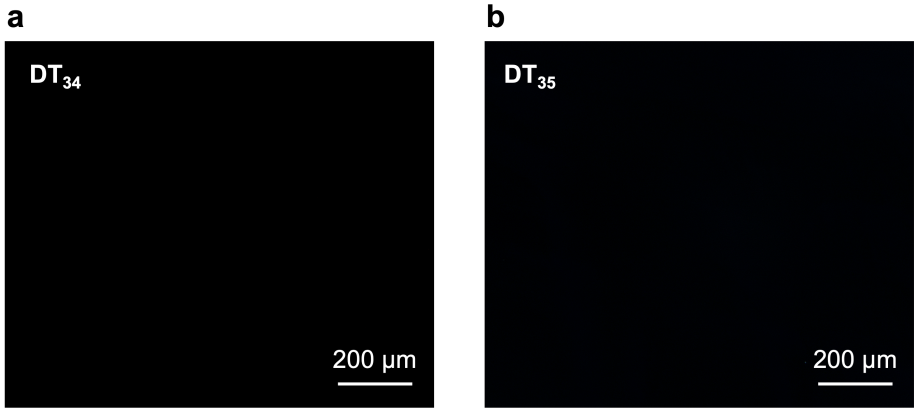

Figure S4. Polarized optical microcopy images of **DT**$_{34}$ and **DT**$_{35}$ at a concentration of 10 mM in dodecane with cover glass.

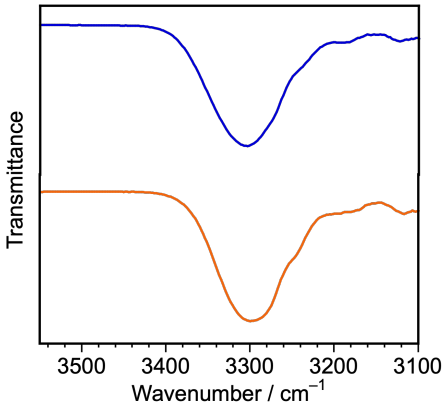

Figure S5. FT-IR spectra of a solution of **DT$_{34}$** (blue line) and **DT$_{35}$** (orange line) at a concentration of 10 mM in dodecane.

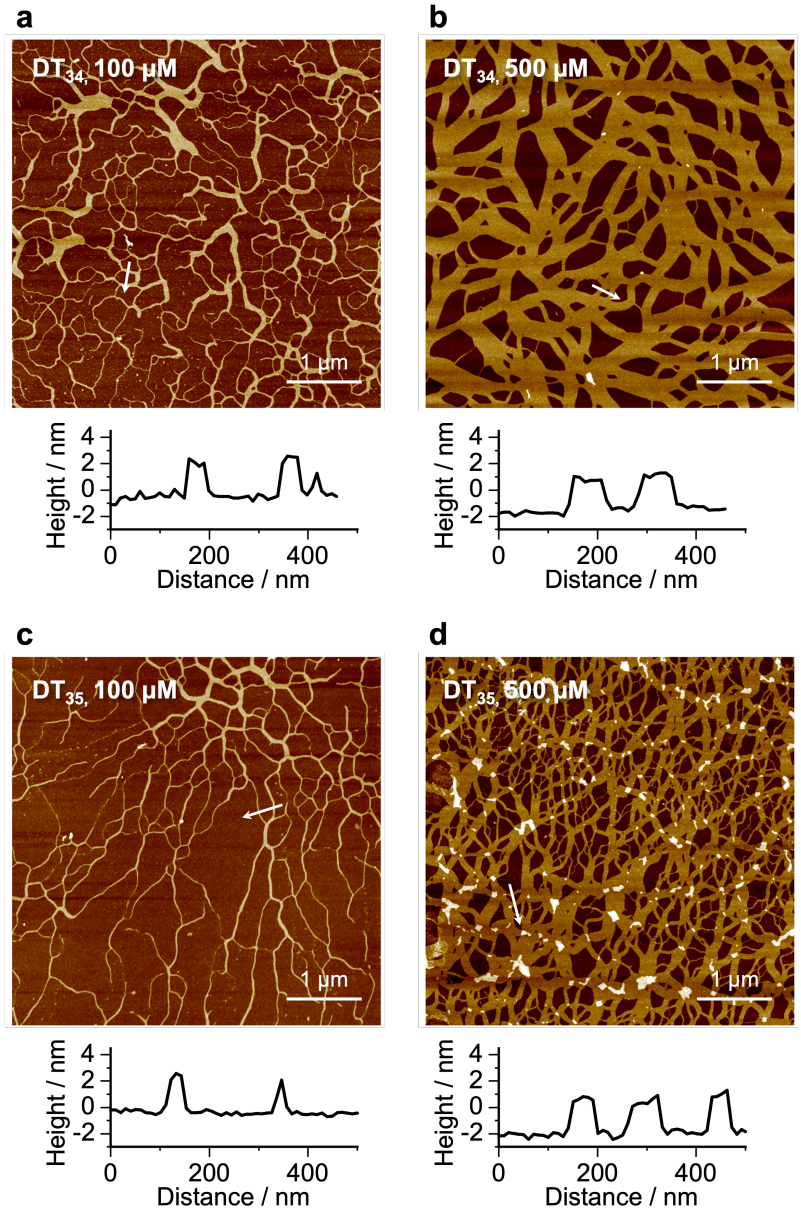

Figure S6. AFM height images of supramolecular polymers consisting of (a, b) **DT$_{34}$** and (c, d) **DT$_{35}$**, spin-coated from dodecane solutions onto silicon wafers (concentrations of (a, c) 10.0×10^{-5} M and (b, d) 50.0×10^{-5} M). Cross-sectional analyses along the white arrows are shown below the corresponding AFM images.

3.2 EQ Model Fitting using Global Fitting Approach

The elongation enthalpy (ΔH_e^0), nucleation penalty (ΔH_n^0), entropy (ΔS) and elongation temperature (T_e) were obtained directly from the cooperative model fitting, while the Gibbs free energy (ΔG^0) for a standard temperature of T = 298 K. A detailed description of the mechanistic foundation of the model is reported in the literature.[S3]

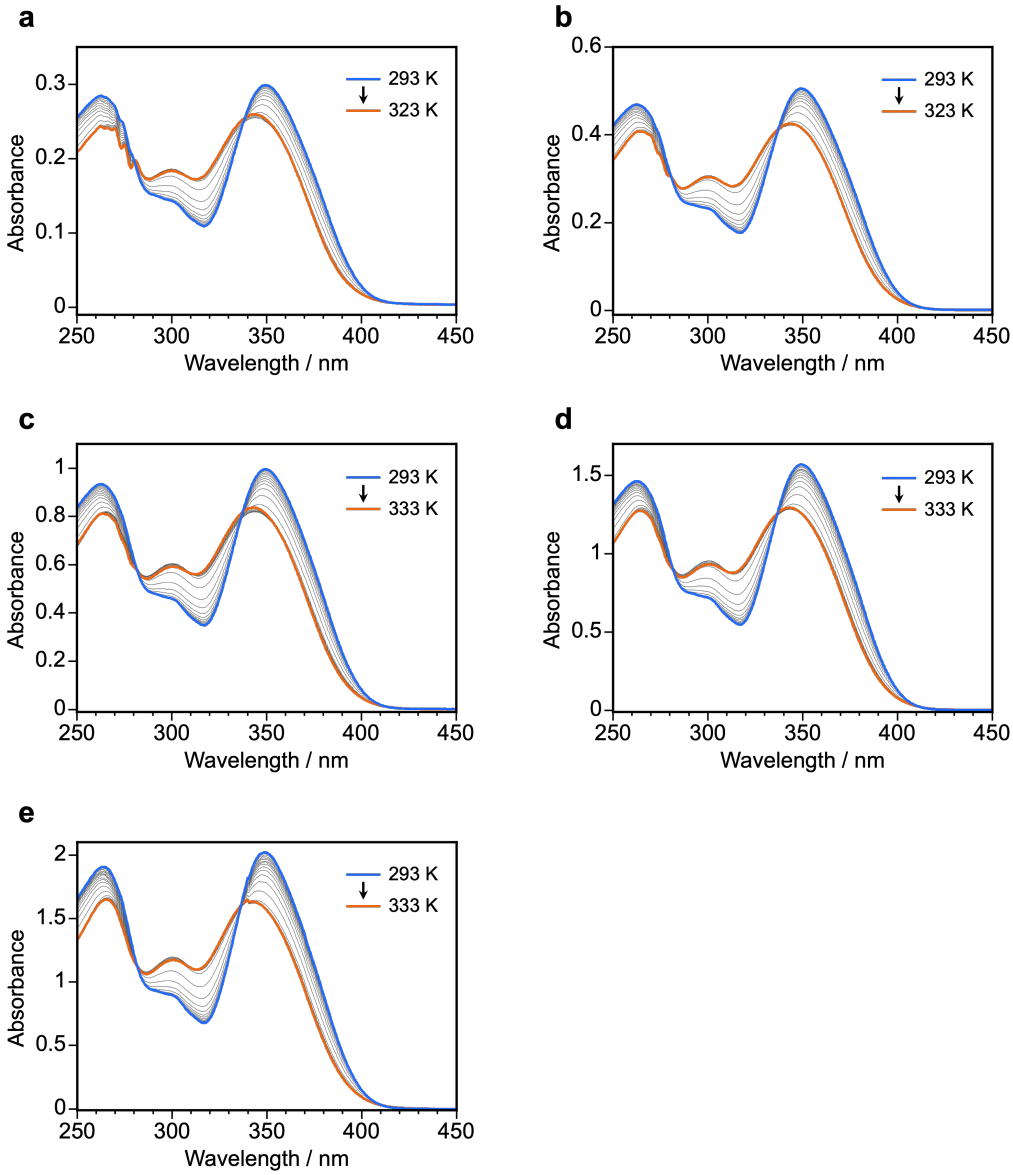

Figure S7. Temperature-dependent UV-vis absorption spectra of **DT$_{34}$** in dodecane at a concentration of (a) 3.0 × 10^{-5} M, (b) 5.0 × 10^{-5} M, (c) 10.0 × 10^{-5} M, (d) 15.0 × 10^{-5} M, and (e) 20.0 × 10^{-5} M upon increasing temperature at a rate of 1 K min^{-1}.

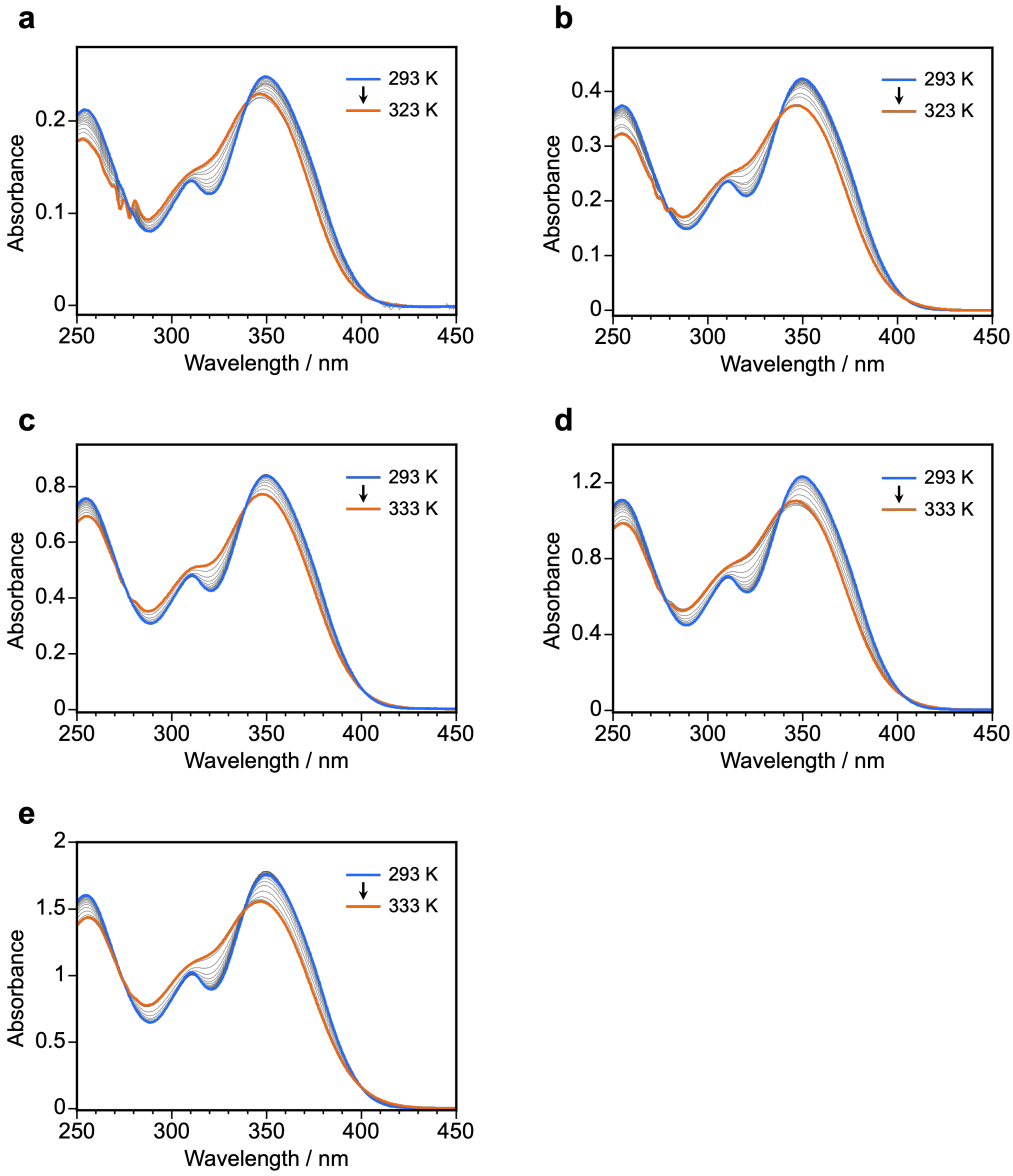

Figure S8. Temperature-dependent UV-vis absorption spectra of **DT_{35}** in dodecane at a concentration of (a) 3.0×10^{-5} M, (b) 5.0×10^{-5} M, (c) 10.0×10^{-5} M, (d) 15.0×10^{-5} M, and (e) 20.0×10^{-5} M upon increasing temperature at a rate of 1 K min^{-1}.

Table S2. Thermodynamic Parameters of **DT$_{34}$** and **DT$_{35}$** Obtained from Temperature-Dependent UV/vis Absorption Spectral Change Fitted by EQ Model Using a Global Fitting Approach

Compound	ΔH_e^0 (kJ/mol)	ΔS (J/mol·K)	ΔG^0 (kJ/mol)[a]	ΔH_n^0 (kJ/mol)
DT$_{34}$	–191.1 (±3.5)	–526.0 (±11.4)	–34.4	–10.61 (±0.62)
DT$_{35}$	–155.9 (±3.9)	–405.0 (±12.4)	–35.2	–11.18 (±0.91)

[a] T = 298 K

3.3 Cooperative Model Fitting of Elongation Process and van't Hoff Plots

The transition temperatures (T_e) were obtained from fitting the elongation regime of the cooperative model.[S4] The thermodynamic parameters were also analyzed by van't Hoff plots.[S4a, S5]

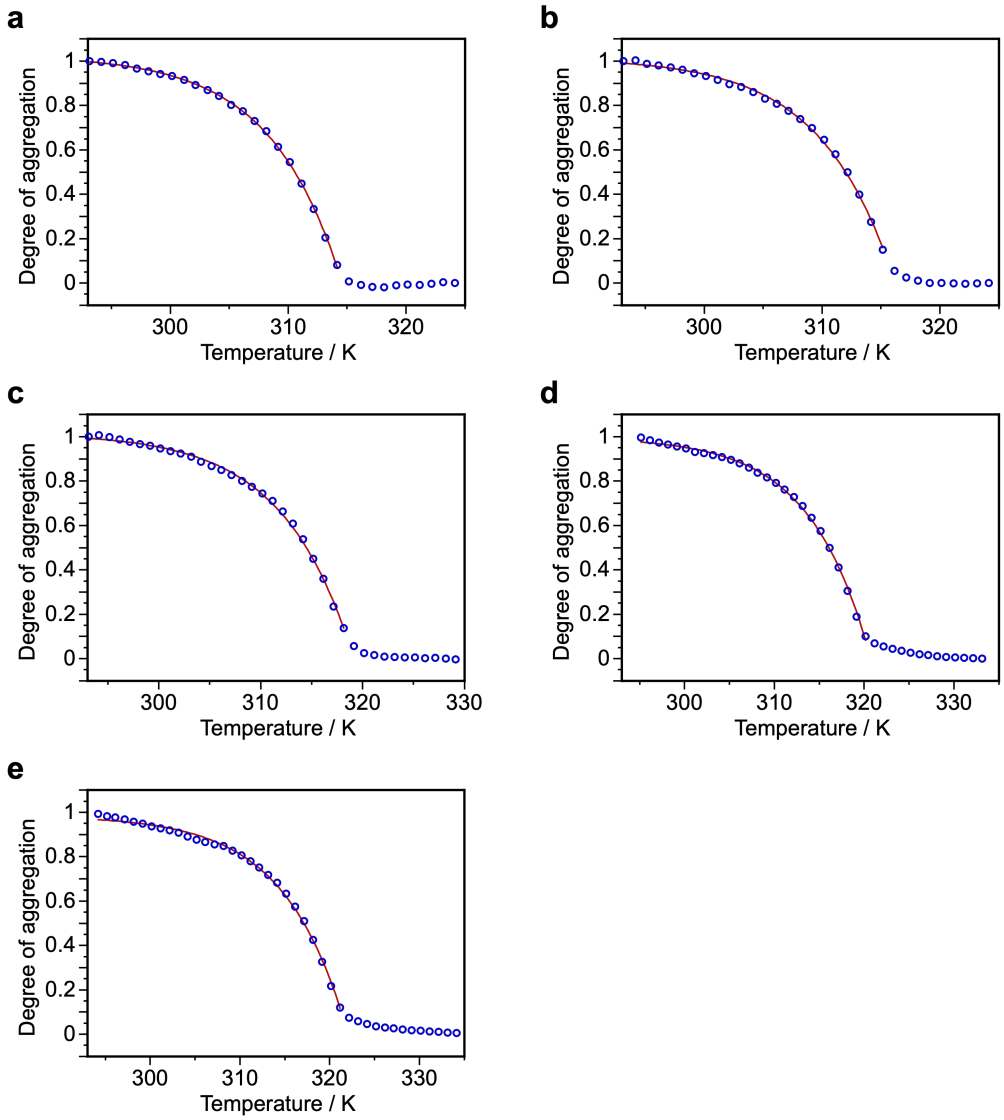

Figure S9. The degree of aggregation of **DT$_{34}$** plotted against the temperature in dodecane at a concentration of (a) 3.0×10^{-5} M, (b) 5.0×10^{-5} M, (c) 10.0×10^{-5} M, (d) 15.0×10^{-5} M, and (e) 20.0×10^{-5} M. The fitting curves were obtained from the cooperative model.

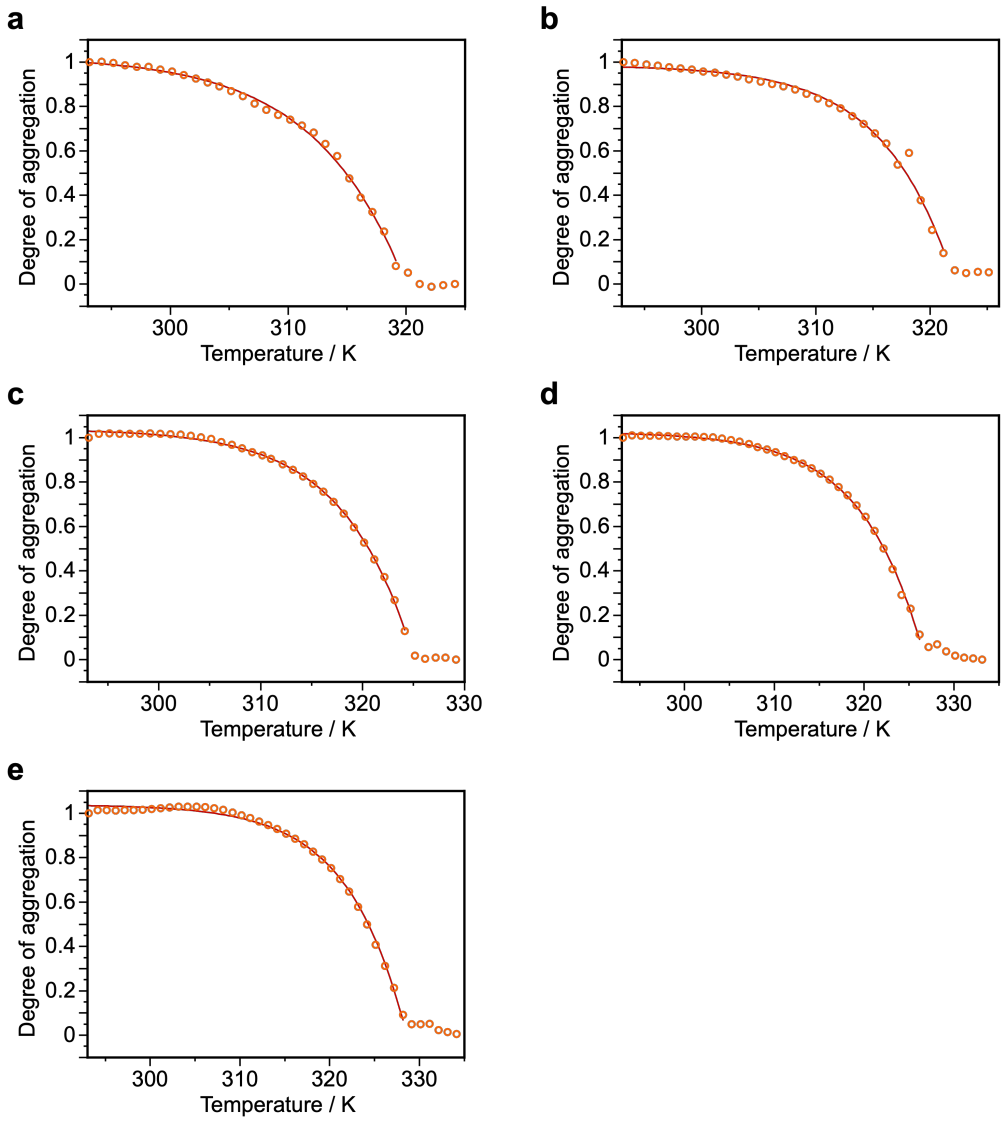

Figure S10. The degree of aggregation of **DT$_{35}$** plotted against the temperature in dodecane at a concentration of (a) 3.0×10^{-5} M, (b) 5.0×10^{-5} M, (c) 10.0×10^{-5} M, (d) 15.0×10^{-5} M, and (e) 20.0×10^{-5} M. The fitting curves were obtained from the cooperative model.

Table S3. Critical Temperatures of **DT$_{34}$** and **DT$_{35}$** Obtained from Temperature-Dependent UV/vis Absorption Spectral Change Fitted by Cooperative Model

	DT$_{34}$	**DT$_{35}$**
c (μM)	T_e (K)	T_e (K)
30	314.6	320.0
50	316.2	322.2
100	319.2	325.1
150	320.6	326.8
200	322.1	328.6

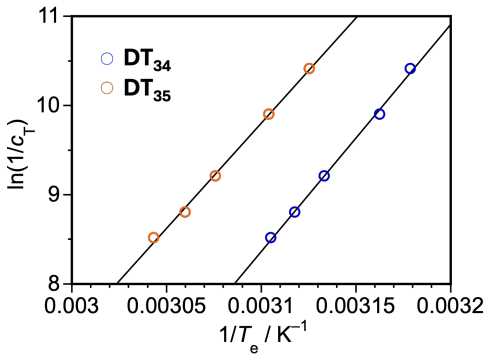

Figure S11. Natural logarithm of the $1/c_T$ (**DT$_{34}$**: blue, **DT$_{35}$**: orange) at $T = T_e$ as a function of $1/T_e$ obtained though the heating curves (in Figure S7 and S8).

Table S4. Thermodynamic Parameters Obtained from van't Hoff Plots

Compound	$\Delta G°$ (kJ/mol)[a]	$\Delta H°$ (kJ/mol)	$\Delta S°$ (J/mol·K)
DT$_{34}$	–36.8	–211.8	–587
DT$_{35}$	–39.2	–196.1	–527

[a] T = 298 K

3.4 Viscoelastic Behavior

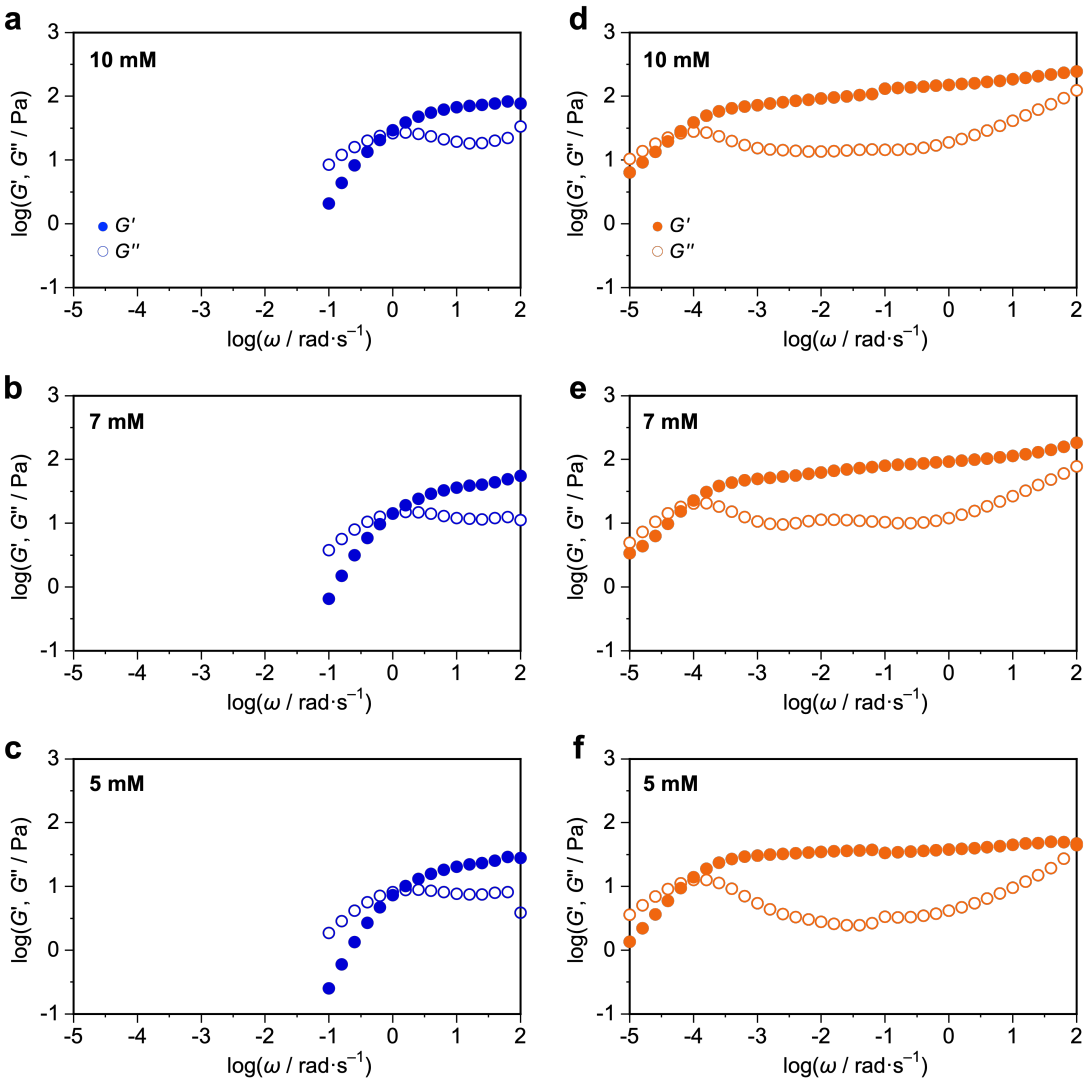

Figure S12. Angular frequency dependence of the storage (G', filled circle) and loss (G'', hollow circle) moduli for (a-c) **DT$_{34}$** and (d-f) **DT$_{35}$** at various concentrations: [**DT$_{34}$** or **DT$_{35}$**] = (a, d) 10 mM, (b, e) 7 mM, (c, f) 5 mM.

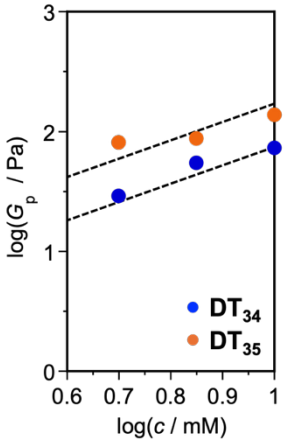

Figure S13. Plateau modulus (G_p) of **DT$_{34}$** (blue) and **DT$_{35}$** (orange) against concentration. The dotted lines show a slope of 1.5.

4. ^{1}H and ^{13}C NMR Spectra

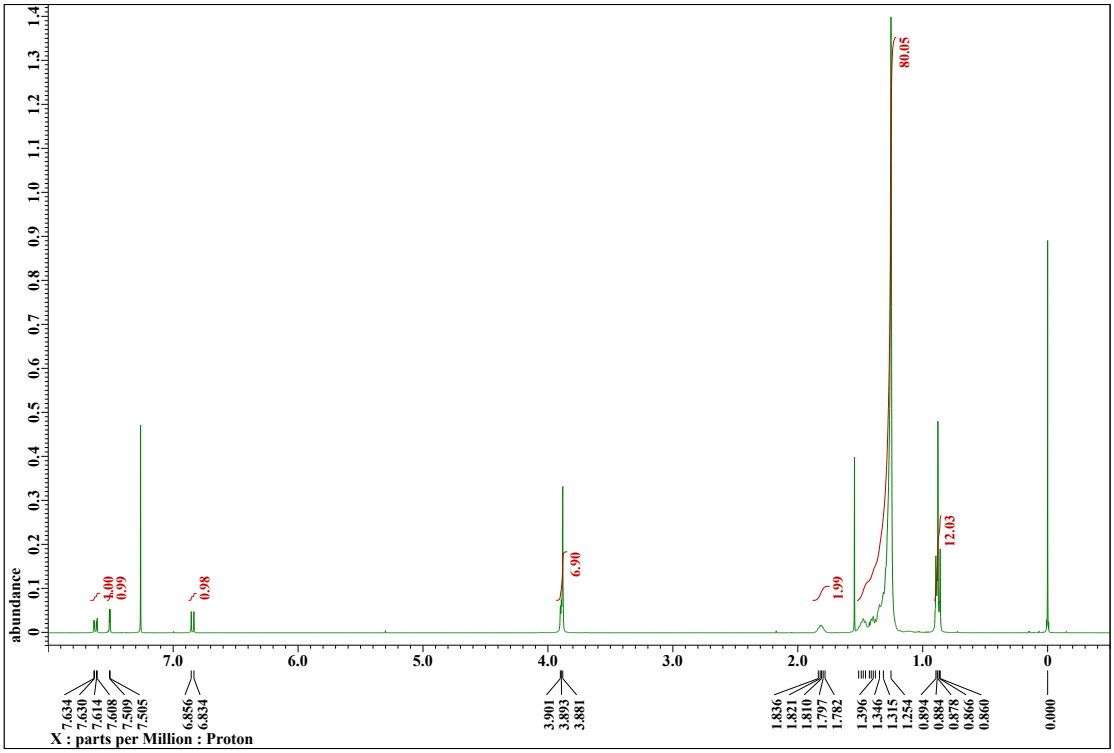

Figure S14. ^{1}H NMR spectrum of **S2** (400 MHz, $CDCl_3$).

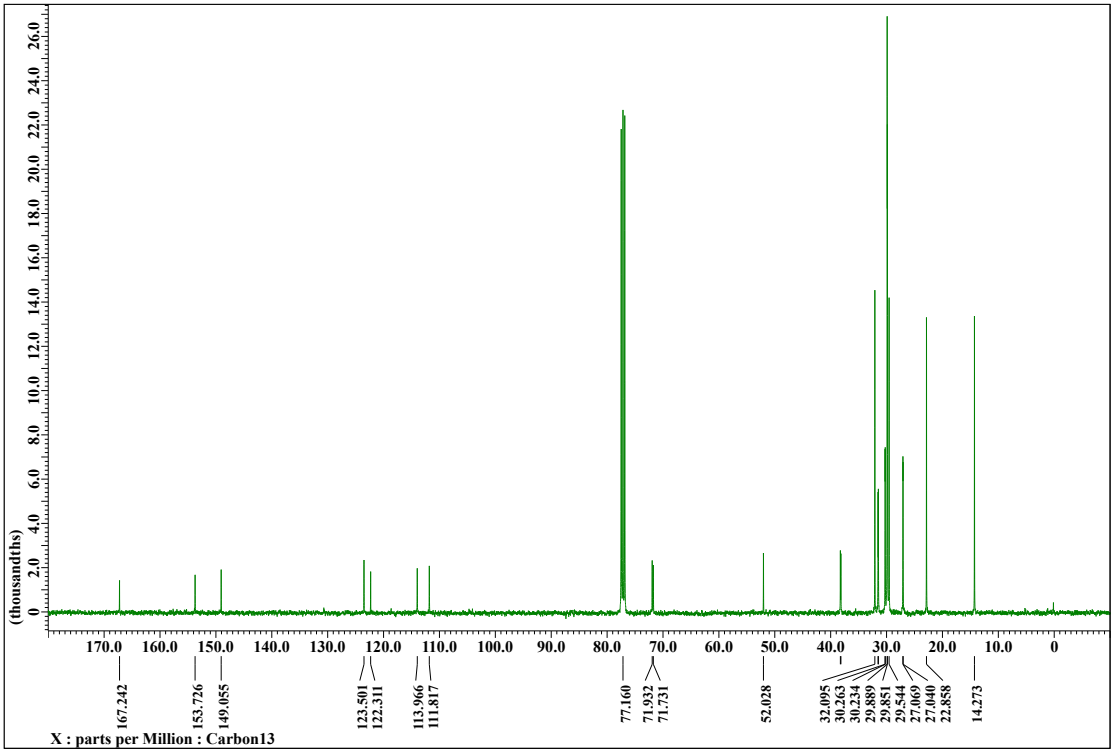

Figure S15. ^{13}C NMR spectrum of **S2** (100 MHz, $CDCl_3$).

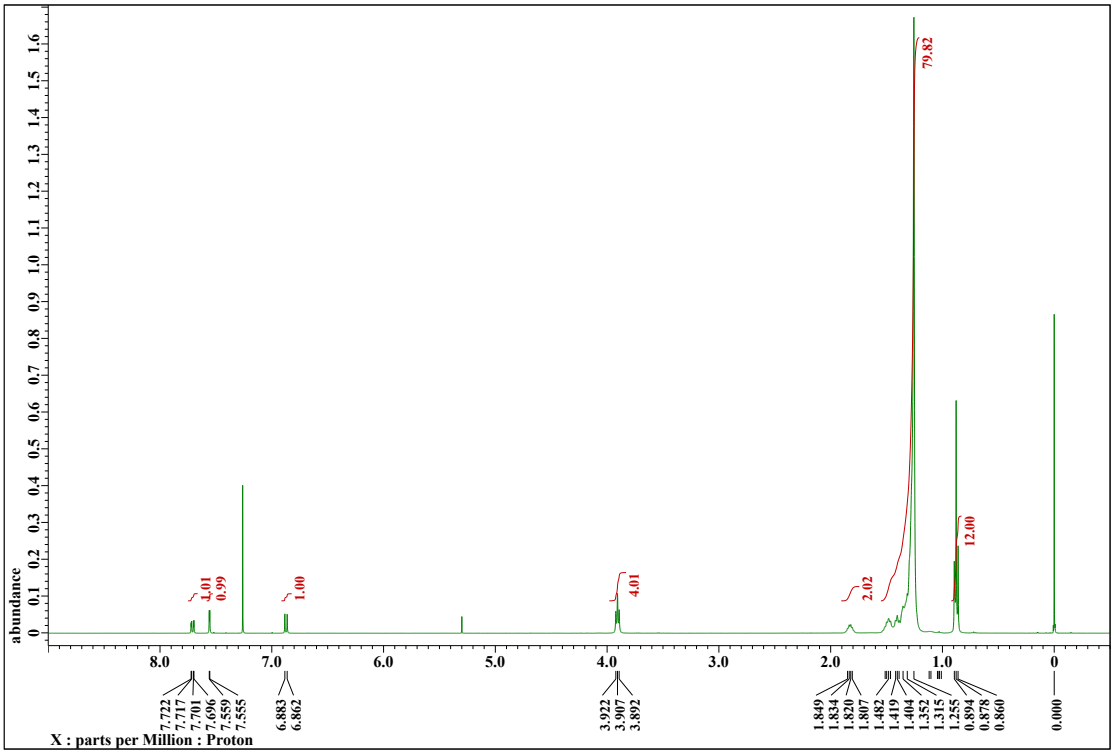

Figure S16. ^{1}H NMR spectrum of **S3** (400 MHz, $CDCl_3$).

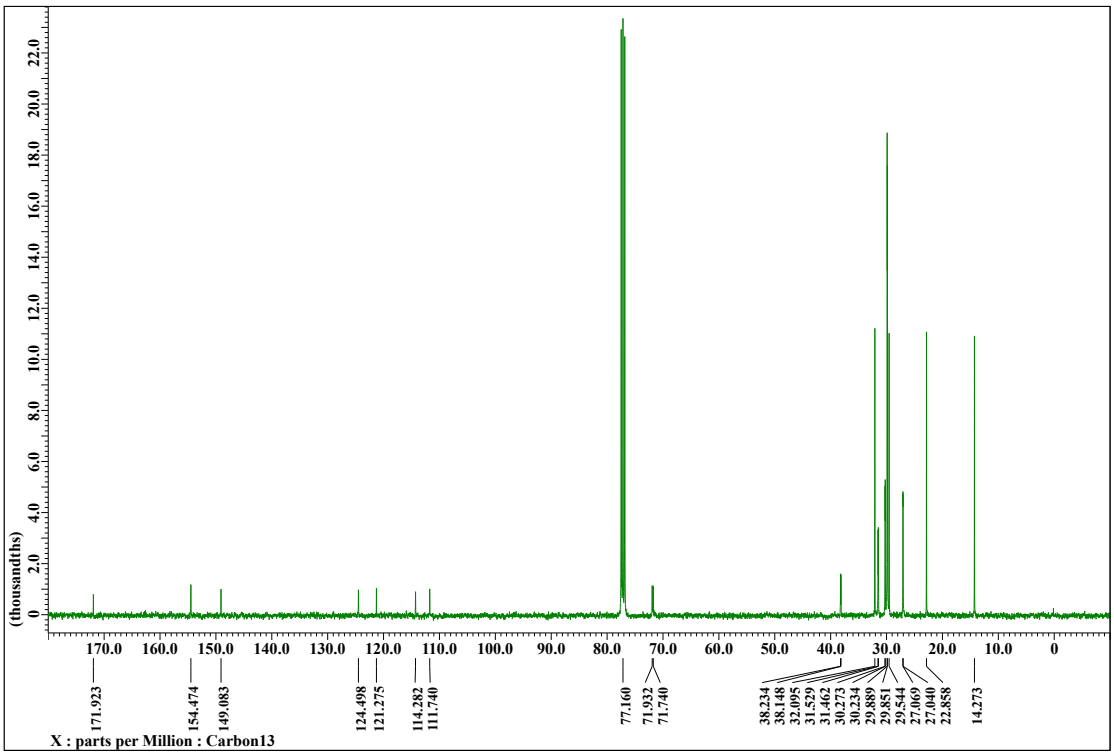

Figure S17. ^{13}C NMR spectrum of **S3** (100 MHz, $CDCl_3$).

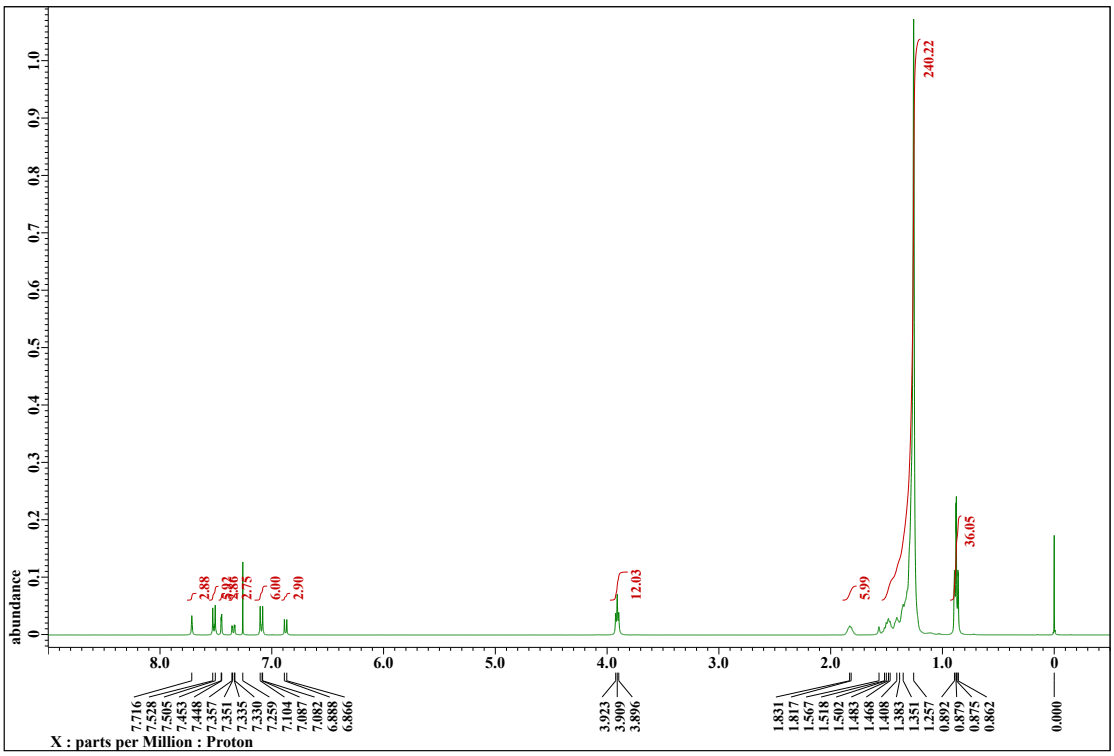

Figure S18. ^{1}H NMR spectrum of **DT$_{34}$** (400 MHz, $CDCl_3$).

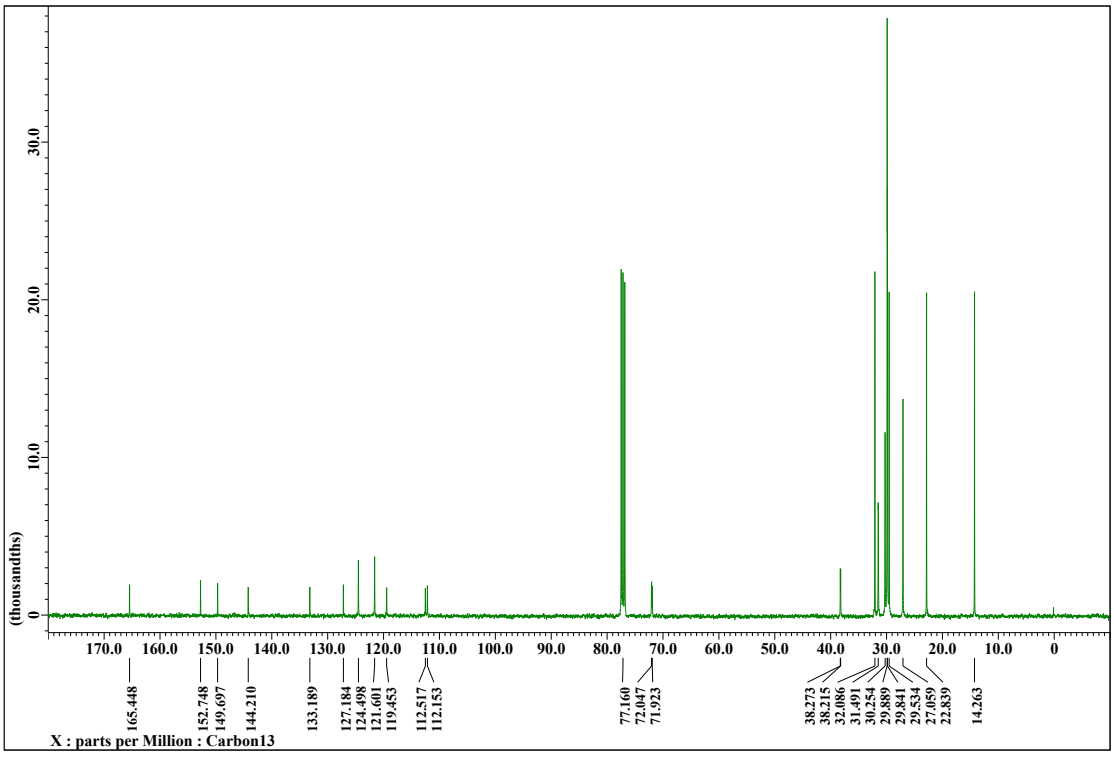

Figure S19. ^{13}C NMR spectrum of **DT$_{34}$** (100 MHz, $CDCl_3$).

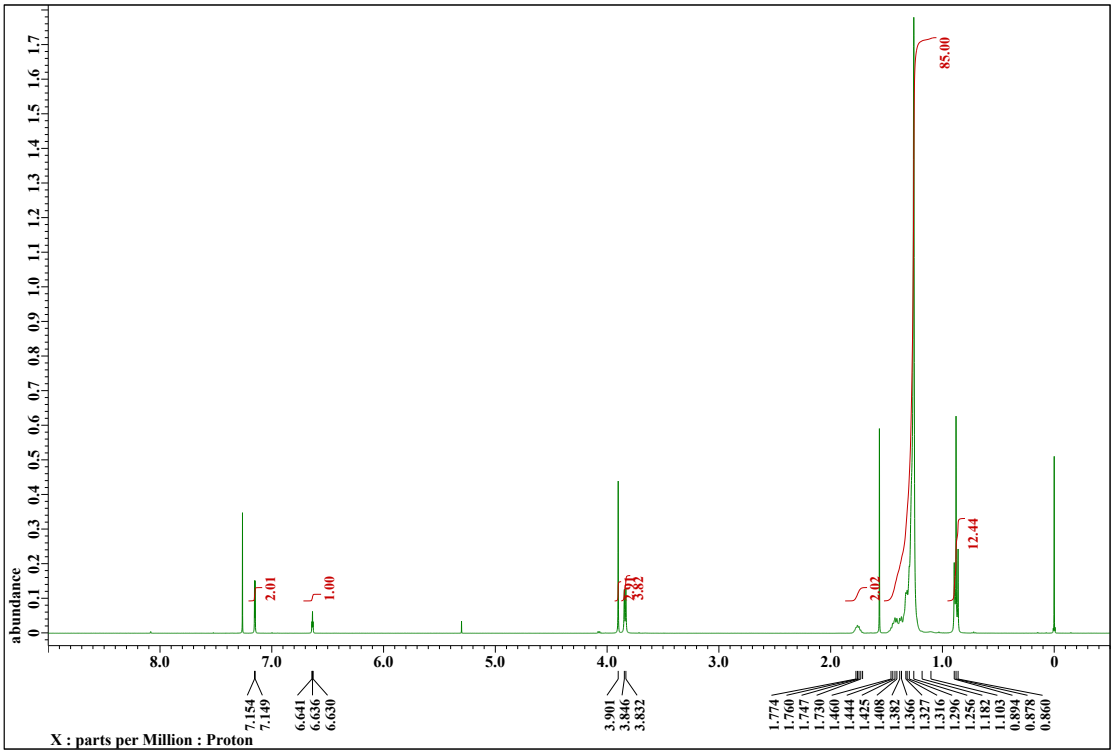

Figure S20. ^{1}H NMR spectrum of **S4** (400 MHz, $CDCl_3$).

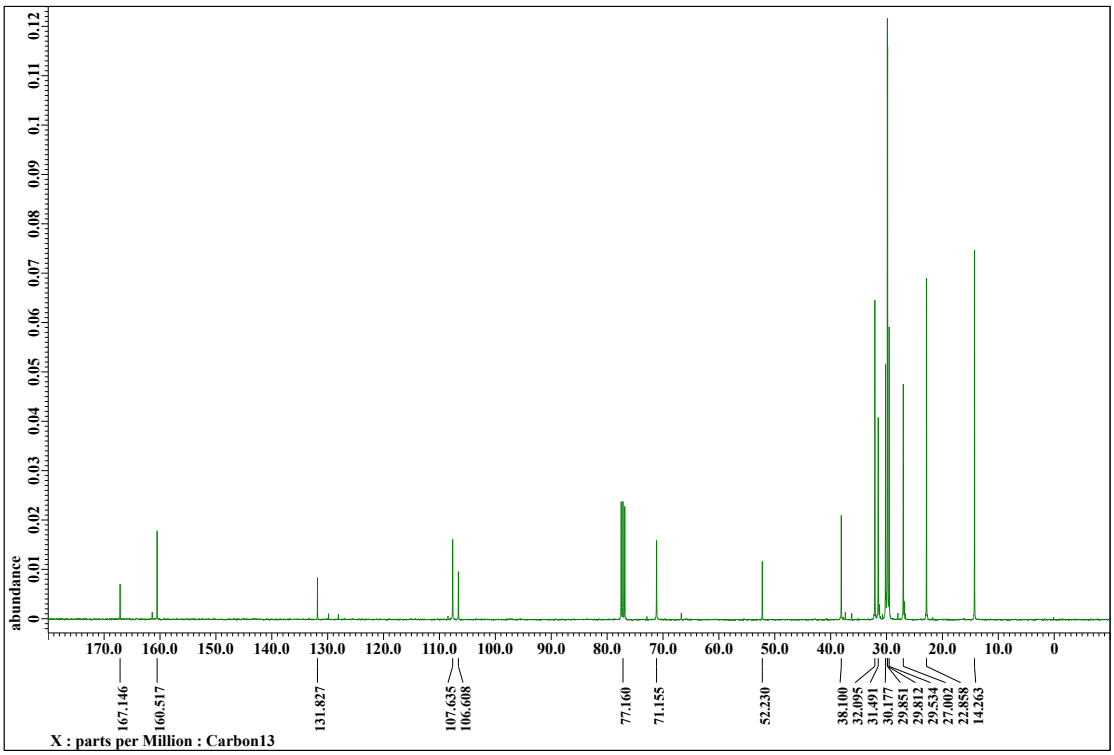

Figure S21. ^{13}C NMR spectrum of **S4** (100 MHz, $CDCl_3$).

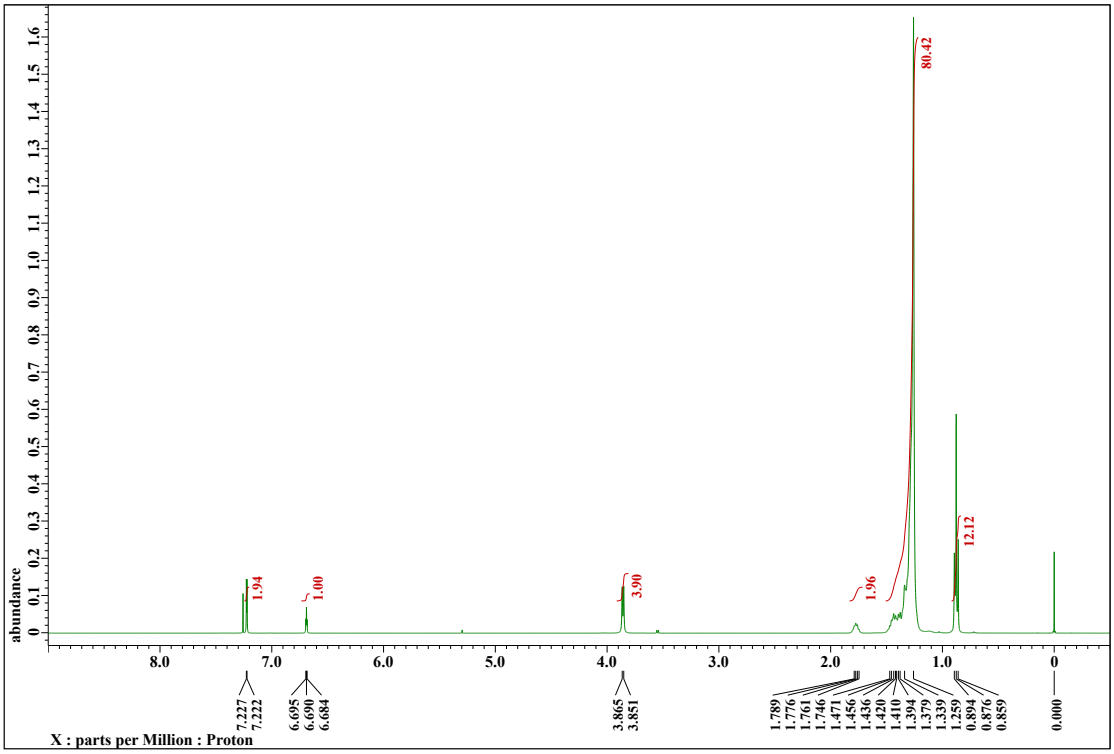

Figure S22. ^{1}H NMR spectrum of **S5** (400 MHz, $CDCl_3$).

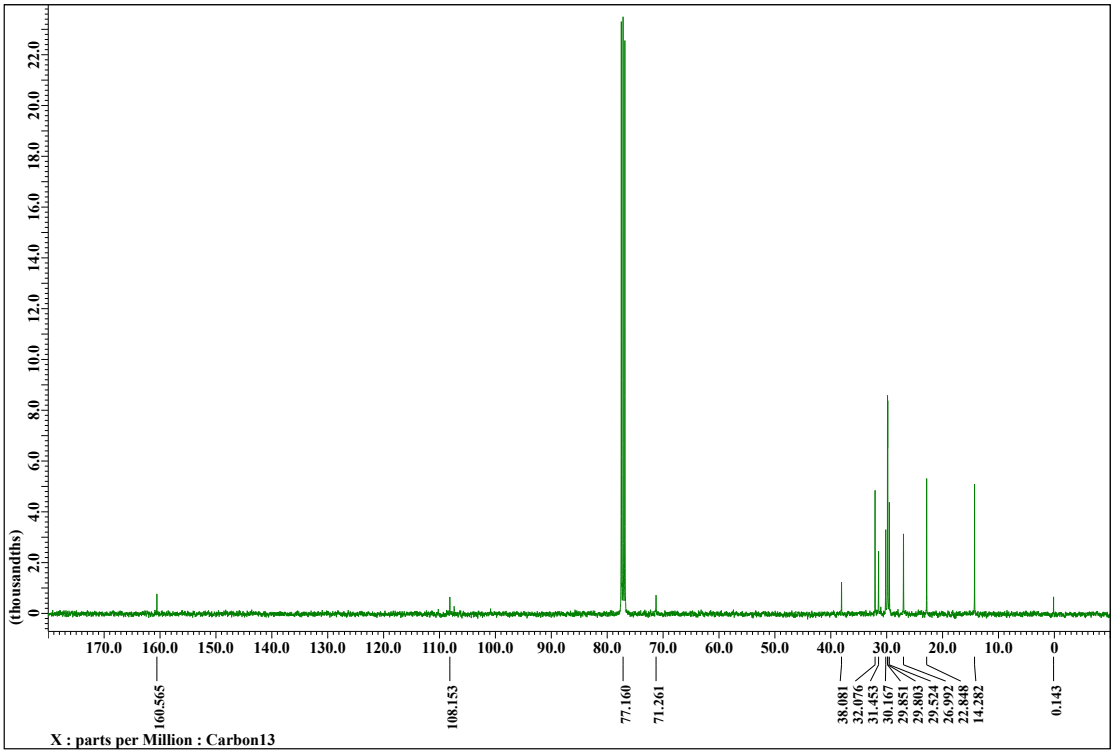

Figure S23. ^{13}C NMR spectrum of **S5** (100 MHz, $CDCl_3$).

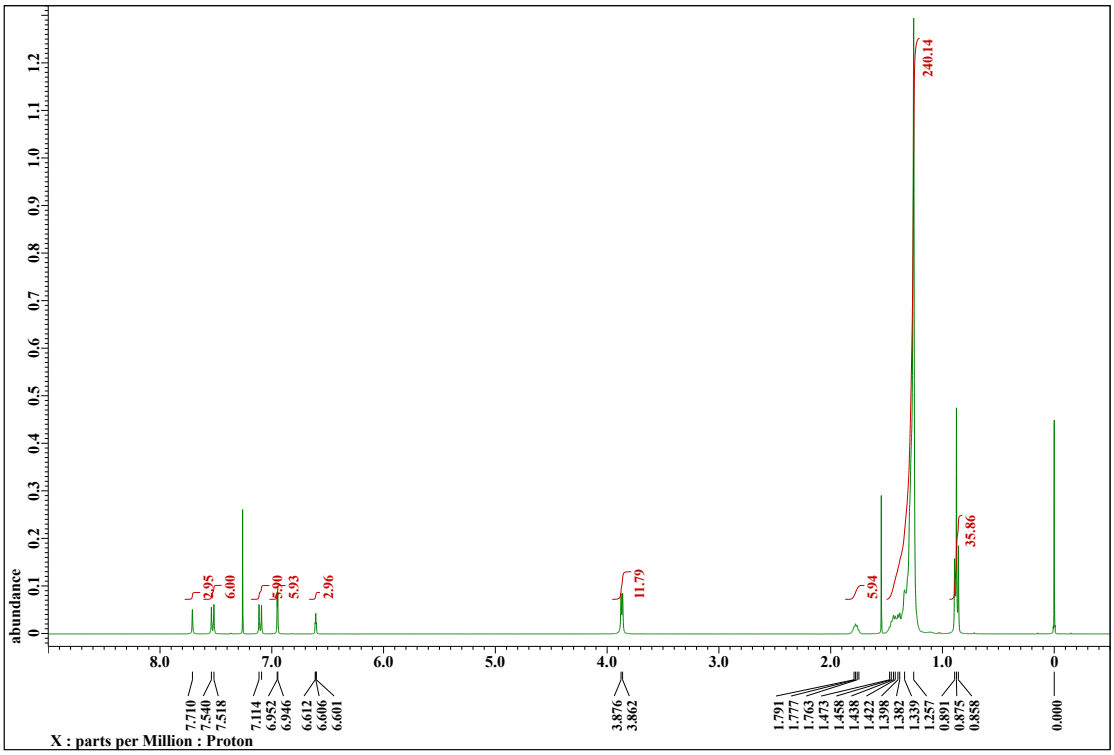

Figure S24. ^{1}H NMR spectrum of **DT$_{35}$** (400 MHz, $CDCl_3$).

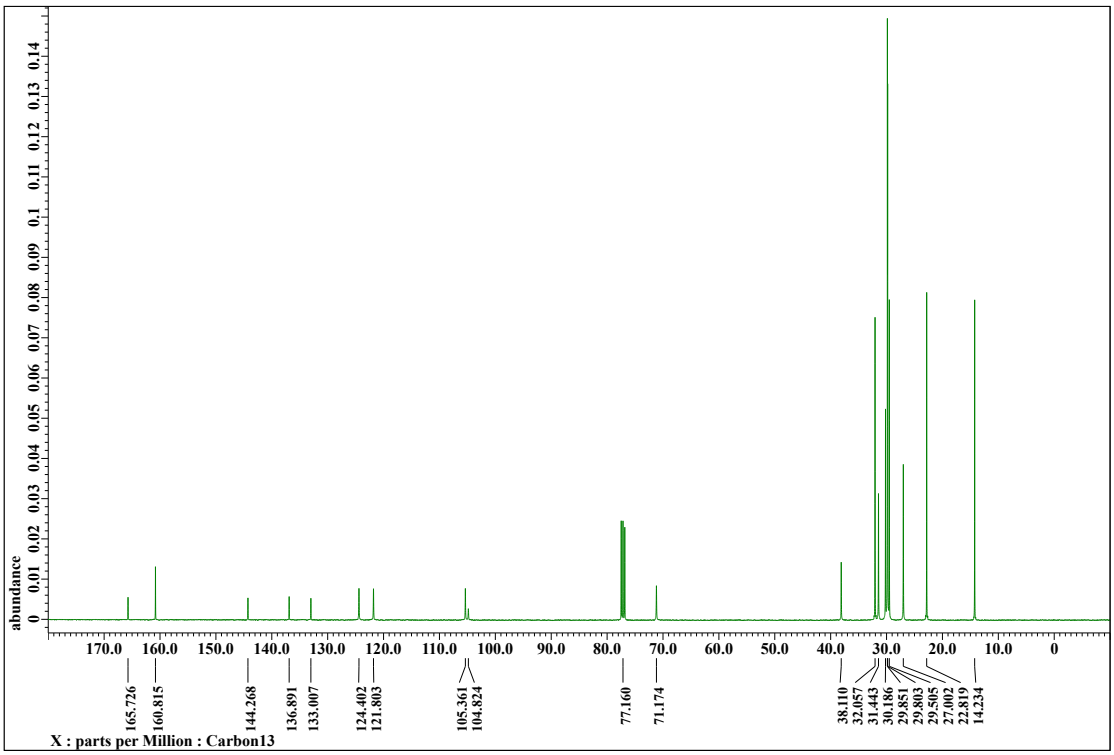

Figure S25. ^{13}C NMR spectrum of **DT$_{35}$** (100 MHz, $CDCl_3$).

5. Supplementary References

S1. A. Tateyama, K. Nagura, M. Yamanaka and T. Nakanishi, Alkyl–π Functional Molecular Gels: Control of Elastic Modulus and Improvement of Electret Performance, *Angew. Chem. Int. Ed.*, 2024, **63**, e202402874.

S2. T. Kim, T. Mori, T. Aida and D. Miyajima, Dynamic propeller conformation for the unprecedentedly high degree of chiral amplification of supramolecular helices, *Chem. Sci.*, 2016, **7**, 6689–6694.

S3. H. M. M. ten Eikelder, A. J. Markvoort, T. F. A. de Greef and P. A. J. Hilbers, An Equilibrium Model for Chiral Amplification in Supramolecular Polymers, *J. Phys. Chem. B*, 2012, **116**, 5291–5301.

S4. (a) P. Jonkheijm, P. van der Schoot, A. P. H. J. Schenning and E. W. Meijer, Probing the Solvent-Assisted Nucleation Pathway in Chemical Self-Assembly, *Science*, 2006, **313**, 80–83; (b) M. M. J. Smulders, M. M. L. Nieuwenhuizen, T. F. A. de Greef, P. van der Schoot, A. P. H. J. Schenning and E. W. Meijer, How to Distinguish Isodesmic from Cooperative Supramolecular Polymerisation, *Chem. Eur. J.*, 2010, **16**, 362–367.

S5. M. M. J. Smulders, A. P. H. J. Schenning and E. W. Meijer, Insight into the Mechanisms of Cooperative Self-Assembly: The "Sergeants-and-Soldiers" Principle of Chiral and Achiral C3-Symmetrical Discotic Triamides, *J. Am. Chem. Soc.*, 2008, **130**, 606–611.